International Journal of Engineering Research & Management Technology
ISSN: 2348-4039
Volume 9, Issue-6 November-December- 2022
Email: editor@ijermt.org www.ijermt.org

THE DENSITY OF STATE OF THE ONE PARTICLE EXCITATION FROM THE SUPERCONDUCTING CONDENSATE STATE

Vijay Kumar Pancholi

Department of physics , M.L.V Government college

Bhilwara, Rajasthan, India

ABSTRACT

We develop a strong-coupling theory of Bose-Einstein condensate-mediated superconductivity in a hybrid system. This system consists of a two-dimensional electron gas in the vicinity of a two-dimensional solid-state condensate of indirect excitons. The electron gas can have either a parabolic spectrum or a relativistic Dirac spectrum. The Eliashberg equations are obtained, and the formulas for the electron pairing self-energy owing to the exchange interaction between electrons that is mediated by a single Bogoliubov excitation (a bogolon) and the bogolon pairs are discovered. Both of these results are shown to be due to the exchange interaction between electrons that is mediated by a single Bogoliubov excitation. In addition to this, we determine the value of the superconducting order parameter and provide an estimate of the temperature at which the superconducting transition occurs. The critical temperature demonstrates the dimensionless coupling constant's linear dependency on the critical temperature. It has been shown that the bogolon-pair-mediated interaction is the preeminent mechanism of electron pairing in hybrid systems in both the weak-coupling and the strong-coupling regimes of operation. We analyze the dependency of the critical temperature of the superconducting transition on the exciton condensate density, and we determine the effective bogolon-electron interaction constant for both parabolic and linear electron dispersions.

Keywords: *Particle Excitation, Superconducting, Condensate*

INTRODUCTION

The disappearance of a sample's static electrical resistance and the ejection of the magnetic field from the inside of a sample are two of the defining characteristics of superconductivity. The theory of superconductivity is the primary focus of this course; nevertheless, we will spend the next chapter talking about some of the fundamental experiments in this field. Utilizing the tools of theoretical physics, our goal is to comprehend the phenomenon of superconductivity. Experiments will be discussed if they inspire specific theoretical notions or if they support or contradict theoretical expectations, but there will not be a systematic examination of the findings of the experiments. There is a connection between the phenomena of superfluidity and Bose-Einstein condensation, which occurs in weakly interacting boson systems. Superconductivity is also connected to these two phenomena. It has been discovered that the commonalities lay more in the efficient low-energy description than in the microscopic particulars. Microscopically speaking, the relationship between superfluidity and superconductivity is the closest one possible due to the fact that both phenomena entail the condensation of fermions. On the other hand, in Bose-Einstein condensates and, of course, in Bose-Einstein condensates, it is bosons that condense. These occurrences will get a cursory examination from us.

As we go on to the microscopic explanation of superconductivity, the first thing we are going to do is investigate the source of the attractive electron-electron interaction that occurs in typical superconductors. Both the Bardeen-Cooper-Schrieffer (BCS) theory of superconductivity and the Cooper instability of the typical Fermi sea will need a knowledge of this information in order to function properly. Now that we have this theory, we will talk about the experimental repercussions, such as how it affects thermodynamics, single-particle tunneling, and nuclear relaxation. After that, we will move on to pair tunneling and the consequences of Josephson. We are going to add the Bogoliubov-de Gennes equation for inhomogeneous superconductors to our theoretical toolbox so that we may enhance our theoretical toolbox. Unconventional superconductors, such as cuprates and pnictides, Andreev scattering and Andreev bound states, and topological superconductors will be the focus of the concluding chapters of this book. The standard content from electrodynamics, quantum mechanics, thermodynamics, and statistics is assumed to be known by students enrolled in this course. In addition to this, we will use the second-quantization formalism, often known as the creation and annihilation operators, which is typically presented in quantum mechanics. An introductory course in solid state physics taken in the past would be beneficial, although it is not necessary. There is no need for previous experience in many-particle theory, and all of the relevant ideas and procedures will be presented (or recapitulated) when they are required.

Even after over a hundred years have passed since the first detection of superconductivity, this phase of matter continues to be one of the most interesting and puzzling there is. The discovery made in 1957 by Bardeen, Cooper, and Schrieffer that superconductivity is a condensate of electron pairs, also known as "Cooper pairs," which are formed as a result of an attractive interaction among electrons allowed us to comprehend what superconductivity is. This interaction is mediated in the superconducting materials that were known up until the middle of the seventies by electron-phonon coupling, which gives birth to Cooper pairs in the most symmetric form, that is, vanishing relative orbital angular momentum and spin singlet configuration (nowadays dubbed s-wave pairing). Following the dissemination of the BCS idea came the commencement of research into several alternate pairing types. Early on, Anderson and Morel, together with Balian and Werthamer, conducted research on superconducting phases that would eventually be known as the A-phase and the B-phase of superfluid He.

In contrast to s-wave superconductors, A- and B-phase superconductors are distinguished by the presence of Cooper pairs that have angular momentum and a spin-triplet structure. In contrast to conventional superconductors, which have the most symmetric Cooper pairs, this event marked the beginning of the period of unconventional superconductivity, which consists of condensates of Cooper pairs with a lesser degree of symmetry. Osheroff, Richardson, and Lee's discovery of superfluidity in offered the world its first example of an atypical Cooper coupling. Other pairing processes, such as those based on van der Waals and spin fluctuation mediated interactions, are plainly not of phononic origin. In addition, 3He is the best example of a highly correlated Fermi liquid, which is characterized by a short-range repulsive interaction that results in significant renormalizations of the quasiparticle mass as well as other variables. The presence of an alternative pairing mechanism as well as high correlation effects are essential components that work together to stop electrons from engaging in traditional s-wave pairing.

The natural goal of finding among solids a system with unconventional Cooper pairing was not satisfied until much later, when at the end of the seventies and beginning of the eighties, two novel classes of strongly correlated materials were found, among which some were superconducting. These novel classes of materials

were the heavy Fermion compounds and the organic conductors. The first category of materials is known as intermetallics, and these are the ones that include rare earth ions. The second category of materials are highly anisotropic conductors that are based on organic units. Although it is not apparent until today which kind of Cooper pairing is achieved in many of these materials, several of them exhibit complicated phase diagrams with multiple distinct superconducting phases, which clearly establishes the unusual character of the material. This information is only available today. Both sorts of materials may either develop superconductivity out of phases that are virtually magnetic or evolve into a magnetically ordered state when subjected to high enough pressure. The beginning of the age of unconventional superconductivity was heralded to a larger community in 1986 when it was discovered that high-temperature superconductivity could be found in cuprate compounds that have a layered perovskite structure.

This system continues to predominate in the field of superconducting research up to the current day. It took a few years, but eventually the cuprates were able to establish their unusual character when it came to partnering. In quasi-two-dimensional systems, Cooper pairs have what is known as a spin singlet-wave structure. In cuprate materials, the significance of magnetism in the context of the extraordinary metallic characteristics and superconductivity is highlighted by the fact that, upon carrier doping, a superconductor develops from an antiferromagnetic Mott insulator. This highlights the crucial role that magnetism plays in the context of these remarkable metallic qualities and superconductivity. In the nineteen-nineties, one of the main techniques in the hunt for novel materials was to focus on the pivotal part that magnetism may play in the phenomenon of unconventional superconductivity. Several Ce-based compounds are striking instances of superconductivity connected with magnetic phases. In these compounds, the superconductivity is coupled with a quantum critical point of an antiferromagnetically ordered state. Surprisingly, superconductivity was also discovered inside a ferromagnetic phase, and this discovery may have some connection with the magnetic quantum phase transition that corresponds to it. Sr2RuO4, whose superconductivity was found in, merits a particular position as an outstanding instance of an unconventional superconductor that results from a highly correlated Fermi liquid phase. This is because Sr2RuO4 is an example of an unusual superconductor.

It is possible to think of it as an analog to He in a variety of different ways, including the pairing symmetry, which is closely connected to the A-phase of the superfluid. Those are only two examples. Over the course of the last decade, a great deal of research has been conducted on a variety of facets of this superconductor. More recently, the superconducting skutterudites, such as PrOs4Sb12, have generated significant attention as novel instances of heavy Fermion materials with multiple superconducting phases. This fascination may be attributed to the fact that these materials have many superconducting phases. Another recent emphasis has been the investigation of superconductivity in materials that have geometrically frustrated crystall lattices. This consists of NaxCoO4 that has been intercalated with water, which has been contemplated as a potential realization of superconductivity on a triangular lattice. Also included in this category is the phenomenon of superconductivity in metals that have a pyrochlor crystal structure, such as and despite the fact that it is unclear whether or not these materials are unusual. In the absence of inversion symmetry, the crystal structure may have an even more significant influence on the superconductivity of the material than it does in the case of frustrated lattices. As we shall see in the next section, invariance under time reversal and inversion are two of the most important symmetries for the production of Cooper pairs.

The finding that some hefty Fermion complexes possess a superconducting property CePt3Si and UIr have reignited the debate on the possibility of superconductivity in systems of this nature. In the course of the last

twenty years, significant progress has been made in the study of unconventional superconductivity, both in terms of our knowledge of the underlying theories and the novel materials that have been discovered. In addition to the remarkable progress that has been made in sample fabrication, which is a necessary accessory for the observation of unconventional superconducting phases that are very sensitive to the effects of material disorder, new methods for the discovery of unconventional superconductors are beginning to yield fruit. These lecture notes discuss a few facets of the area of unconventional superconductivity as well as recent advances in the field. This summary naturally excludes some details, and the perspective presented here is colored by the preferences of the presenter.

Real-Time Spectroscopy of the Superconducting Gap Dynamics

In order to study the dynamics of light-induced suppression and recovery of the superconducting state in real-time, the most popular method is to employ a technique known as pump-probe spectroscopy. Excitation (pump) and probing (probe) the induced changes in optical constants as a function of time delay between the two are accomplished using femtosecond optical pulses that have the same photon energy. This is the simplest form. The vast majority of the early experiments were carried out using this setup. Although the photo-induced changes at optical (probe) frequencies do reflect, via Kramers–Kronig relations, the photo-induced changes and dynamics of the low-energy excitation spectrum (for example, the superconducting gap), probing the gap dynamics using far-infrared (THz) pulses or with photoemission is much simpler to interpret. This is because the photo-induced changes and dynamics of the low-energy excitation spectrum are related to each other.

Induced Dynamics of the Superconducting Gap in NbN

Near-infrared pump THz-probe spectroscopy was used to analyze thin NbN thin films that were deposited on MgO substrates. The dynamics of the gap after stimulation with a 50 fs near-infrared (800 nm) pulse may be analyzed after linear THz spectroscopy investigations, during which the temperature dependence of the superconducting gap is retrieved using the fit to the complex optical conductivity. After optical stimulation, the time evolution of the SC state as a function of time delay, t, was investigated by either directly measuring spectrally resolved or by measuring the spectrally integrated response by monitoring the time evolution of the induced changes in the transmitted electric field, respectively. Both of these methods were used to study the time evolution of the SC state. This latter technique is especially helpful for the analysis of dynamics when the excitations are relatively modest. Since films have a uniform thickness throughout their whole surface, they experience uniform excitation. Reflectivity and transmission at 800 nm (pump) may be used to calculate the absorbed energy density, which is denoted by the symbol A (in units of meV per unit cell volume, meV/ucv).

Superconducting State Recovery Dynamics in the Limit

In the earlier subsections, we were primarily concerned with the dynamics that take place at low temperatures, also known as for Now we will discuss the behavior that occurs close to the limit. As was shown in studies that were conducted rather early on, the real-time response of the current–voltage characteristic of a tunnel junction to rapid laser pulses showed the abnormal slowing down of relaxation upon getting closer to the target value. This may be understood by thinking about the relaxation in terms of the Ginzburg-Landau theory of the second-order phase transition. Considering this will lead to the correct interpretation. In this case, the restoring force is calculated using the derivative of the free energy with respect to the order parameter, which

results in a divergence of the free energy. Schmid and Schoen came up with an equation to represent the dependency of the amount of time it takes for the superconducting state to recover when they assumed that the phonons were in a condition of thermal equilibrium.

OBJEACTIVES

1. The study We develop a strong-coupling theory of Bose-Einstein condensate-mediated superconductivity.

2. The study the critical temperature reveals its linear dependence on the dimensionless coupling constant.

RESEARCH METHODOLOGY

Let us imagine a hybrid system in which a layer of a Bose-Einstein condensate (BEC) and a layer of a two-dimensional electron gas (a 2DEG) are in close proximity to one another in the z direction (we use the identical setup as in publications cited in the previous sentence). Indirect excitons are used to represent the bosonic subsystem, and it was only recently discovered that these excitons may create a BEC. Indirect excitons are made up of electrons and holes that are located in n- and p-doped layers that are geographically distant from one another along the z axis. Materials such as MoS2 or WSe2 may be used to create these layers, which are then separated by many layers of hexagonal boron nitride (hBN). Layers of spin and exciton gas are spatially separated by a hBN layer, as is the 2D electron gas, which is characterized by the field operator (r) with the position vector r. The coupling between the electrons and the indirect excitons is provided by the Coulomb interaction.

$$\mathcal{H} = \sum_{\sigma} \int d\mathbf{r} \int d\mathbf{R}\, \Psi_{\sigma}^{\dagger}(\mathbf{r})\Psi_{\sigma}(\mathbf{r})g(\mathbf{r}-\mathbf{R})\Phi^{\dagger}(\mathbf{R})\Phi(\mathbf{R}),$$

where R denotes the position vector of the exciton's center-of-mass motion with respect to the plane. In this scenario, we focus on the situation in which the majority of excitons are located in the ground state (in BEC). The exciton field operator may thus be written as where nc is the condensate density and is the field operator for noncondensed excitons when the system is in the domain of weakly interacting particles. We may determine the Hamiltonian for the one-bogolon (1b) and bogolon-pair-mediated interactions below by using the Fourier and Bogoliubov transformations. For the sake of simplicity, we will restore these constants once we have found the Hamiltonian)

$$\mathcal{H}_1 = \frac{\sqrt{n_c}}{L} \sum_{\mathbf{kp}\sigma} g_{\mathbf{p}}[(v_{\mathbf{p}} + u_{-\mathbf{p}})b_{-\mathbf{p}}^{\dagger} + (v_{-\mathbf{p}} + u_{\mathbf{p}})b_{\mathbf{p}}]c_{\mathbf{k}+\mathbf{p},\sigma}^{\dagger},$$

$$\mathcal{H}_2 = \frac{1}{L^2} \sum_{\mathbf{kpq}\sigma} g_{\mathbf{p}}[u_{\mathbf{q}-\mathbf{p}}u_{\mathbf{q}}b_{\mathbf{q}-\mathbf{p}}^{\dagger}b_{\mathbf{q}} + u_{\mathbf{q}-\mathbf{p}}v_{\mathbf{q}}b_{\mathbf{q}-\mathbf{p}}^{\dagger}b_{-\mathbf{q}}^{\dagger}$$
$$+ v_{\mathbf{q}-\mathbf{p}}u_{\mathbf{q}}b_{-\mathbf{q}+\mathbf{p}}b_{\mathbf{q}} + v_{\mathbf{q}-\mathbf{p}}v_{\mathbf{q}}b_{-\mathbf{q}+\mathbf{p}}b_{-\mathbf{q}}^{\dagger}]c_{\mathbf{k}+\mathbf{p},\sigma}^{\dagger}c_{\mathbf{k},\sigma},$$

We ignore the idiosyncrasies of the exciton's internal motion, which refers to the relative motion of the electron and hole inside the exciton, so that we may obtain an analytical form of the electron-exciton interaction. The exciton binding energy is often rather high in monolayers of transition-metal dichalcogenides; in certain cases, it may even be higher than the temperature of room temperature. Therefore, it is a logical assumption to make that each individual exciton is in its ground state with regard to its relative electron-hole motion, and the only motion that plays a crucial role is the motion of the exciton's center of mass. The electron-exciton interaction in direct space thus yields the following readings.

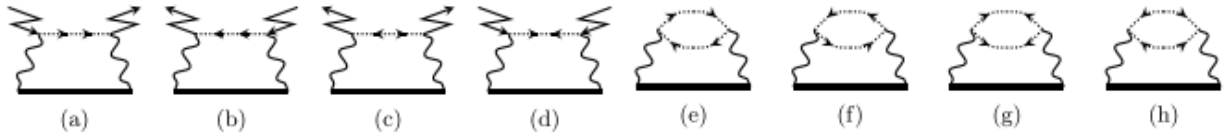

FIG. 1. Electron self-energy diagrams. The double solid lines stand for the Green's functions of an electron Gˆ in Eq. (10). The zigzag lines denote the condensate particles. (Thus, each zigzag line gives the factor √nc). The dotted lines represent bogolons (the particles excited from the condensate). The wiggly lines stand for the electron-exciton interaction gp. Panels (a)–(d) correspond to the 1b process [Eq. (19)], and panels (e)–(h) correspond to the 2b process [Eq. (20)]. Physically, the diagrams in (a)–(d) describe the excitation of a condensate particle to a noncondensed state by a moving electron, whereas (e)–(h) describe the condensate polarization due to the moving electron.

Then, the polarization operator simplifies to.

$$\mathcal{P}^0(\mathbf{p}, i\omega_m) = \frac{-\kappa^2 n_c^2}{L^4} \sum_{\mathbf{q}} \frac{1}{\omega_{\mathbf{q}-\mathbf{p}}\omega_{\mathbf{q}}} \frac{\omega_{\mathbf{q}} + \omega_{\mathbf{q}-\mathbf{p}}}{\omega_m^2 + (\omega_{\mathbf{q}} + \omega_{\mathbf{q}-\mathbf{p}})^2},$$

and the self-energy can be rewritten in the form,

$$\hat{\Sigma}_{2b}(\mathbf{k}, ip_k) = \frac{-1}{\beta} \sum_{\mathbf{p},n} g_{\mathbf{k}-\mathbf{p}}^2 \mathcal{P}^0(\mathbf{k}-\mathbf{p}, ip_k - ip_n) \times \sigma_3 \hat{G}(\mathbf{p}, ip_m)\sigma_3.$$

Already, we have provided evidence to show that the self-energy contribution brought on by the 2b process is predominating. Since all of these terms appear in the perturbative expansion where the small parameter is the electron-exciton interaction strength, we would like to point out that all other terms, such as three- and four- (and more) bogolon-mediated processes, offer lower contributions. This is something that we would want to point out.

DATA ANALYSIS

In this part of the chapter, we will apply the Eliashberg theory to many distinct types of hybrid systems. In specifically, we look at DEG in the case of parabolic dispersion and the electron gas in the case of linear dispersion. To begin, let us try to make the Eliashberg equations as easy to understand as possible by applying the following approximations: We assume that the anisotropy of the Fermi surface is not very strong and, as a result, make use of the isotropic version of the Eliashberg equations. This is because the majority of the

superconducting pairing takes place within a very small energy window close to the Fermi surface (FS). Then, for the sake of brevity, we may rename the scalar functions as follows:

Let us now take into consideration a DEG with a linear dispersion in, for example, a graphene layer. For the sake of simplicity, we will ignore the spinor structure of the wave function and assume that we are dealing with the doped graphene with the Fermi energy being suitably far away from the Dirac point. In addition, we shall not take into consideration the contributions made by the various valleys. Because a large nonzero wave-vector significantly suppresses the interaction, this approximation may be considered accurate.

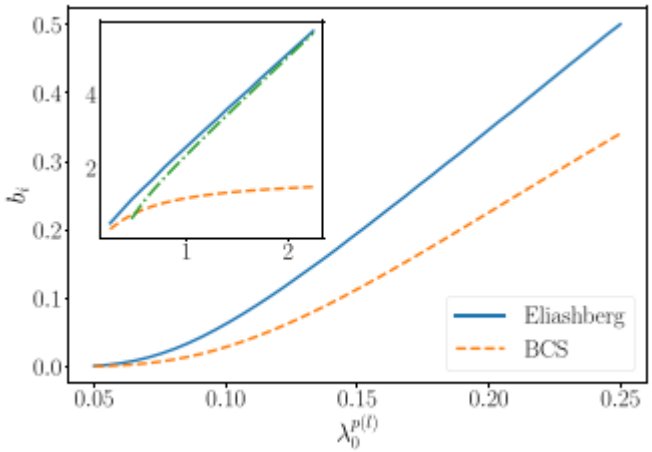

Fig. 2. Dimensionless critical temperature bi as a function of the dimensionless coupling constant λp(l) 0 . The main plot corresponds to the case of small λp(l) 0 . The inset shows the general case of arbitrary λp(l) 0 . Blue solid line: the results of the calculation by the eliashberg equations with be = πt sk f ; yellow dashed line: the results

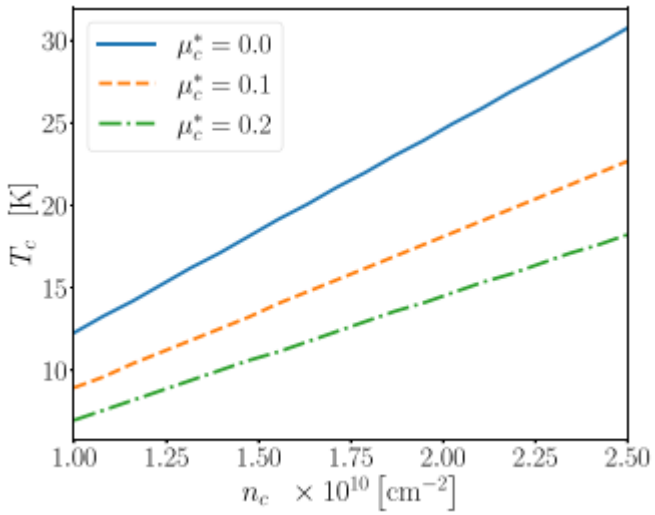

FIG. 3. The critical temperature of the SC transition as a function of condensate density calculated using the Eliashberg theory for different values of dimensionless Coulomb interaction strength We used the parameters typical for mos2: the electron effective mass me = 0.46m0 and exciton effective mass M = m0 with the free-electron mass m0; the dielectric permittivity = 4.89; the interlayer sep

The theories are starting to come into clearer focus. In the asymptotic limit, the dependence of the Eliashberg critical temperature on the coupling coefficient 0 is almost linear. This is the result of the asymptotic limit. This kind of reliance was not characteristic of the ordinary superconductors that were investigated in the early research that led to the discovery of the dependence Tc within the context of the Einstein model. The peculiarities of the angular dependence of the integral in may be seen as the cause of this linear behavior, which can be viewed as the outcome. The almost linear relationship that we observe may also be confirmed analytically if we only consider the leading order of (see the details in Appendix D) as the lower boundary estimate of the critical temperature. This allows for a more precise determination of the temperature at which the critical point is reached. This is a reading of the asymptotic behavior.

Let us now discuss the remaining assumptions that were used in the computations that we performed. First, in order to obtain) in addition to the conventional approximations that were covered in Section IV, we additionally estimated the exciton-electron interaction by using the formula gp = e2 0d/2 0. This was done in addition to the standard approximations. A simplification of this kind is acceptable provided that kf d and kf both equal . Because of this assumption, there is a limit placed on the highest permissible value of ne for the distances d and l that are taken into consideration. If the distances between d and are measured in nanometers, then the electron density should be denoted by ne. Second, the polarization operator that we examine here does not contain the Nq terms, as was previously noted in the preceding paragraph.

Since these contributions produce an integral truncation from L1 BEC to kf/2, these terms are very insignificant when the size of the condensate LBEC is small, as was shown in the study conducted within the framework of the BCS theory. This was the case because these terms give an integral truncation. To put it another way, we determine the lower limit for the SC gap as well as the Tc. Because we are interested in the critical temperature of the SC transition, we gave consideration to the Green's function for electrons while also taking into account the finite temperature. In the BCS theory, the nonzero factors in contribute to a nonmonotonous temperature dependency, and they only serve to boost the critical temperature. This is something that has been pointed out in previous publications on bogolon- and phonon-mediated superconductivity. As a result, the simplifications we made were of a technical character, and as a consequence, they did not significantly alter either our findings or our conclusions. In conclusion, we would like to address some of the concerns that have been raised about the relevance of our findings within the framework of the Hohenberg-Mermin-Wagner theorem. This theorem posits that there is no such thing as long-range order in infinitely many two-dimensional systems operating at finite temperatures.

CONCLUSION

We developed the Eliashberg theory of the Bose condensate-mediated superconductivity in hybrid two-dimensional Bose-Fermi systems and showed that the bogolon-pair-mediated pairing of electrons represents the dominant mechanism not only in the weak-, but also in the strong-coupling regime. On the other hand, single-bogolon pairing is suppressed and, as a result, does not play any significant role in the phenomenon. We began by developing an analytical expression for the self-energy of electrons in a two-dimensional material as a result of their interaction with bogolons. Following that, we calculated the electron-bogolon coupling constant in the cases of parabolic and linear electron dispersions and presented the corresponding estimations of the critical temperature of superconducting transition, which turns out to be relatively high. It has been shown that the critical temperature of the superconducting transition relies on the dimensionless coupling constant in a linear fashion, which is not something that is typical for superconductors that are

traditionally used. We anticipate that our theory and the estimates will have an influence on research fields such as mesoscopic superconductivity, innovative two-dimensional Dirac materials, and low-dimensional superconductors.

REFERENCES

1. J. Bardeen, L. N. Cooper, and J. R. Schrieffer, Microscopic theory of superconductivity, Phys. Rev. 106, 162 (1957).
2. J. Bardeen, L. N. Cooper, and J. R. Schrieffer, Theory of superconductivity, Phys. Rev. 108, 1175 (1957).
3. J. P. Carbotte, Properties of boson-exchange superconductors, Rev. Mod. Phys. 62, 1027 (1990).
4. P. B. Allen and B. Mitrovic, Theory of superconducting ´ Tc, Solid State Phys. 37, 1 (1983).
5. A. Migdal, Interaction between electrons and lattice vibrations in a normal metal, Sov. Phys. JETP 7, 996 (1958).
6. G. M. Eliashberg, Interactions between electrons and lattice vibrations in a superconductor, Sov. Phys. JETP 11, 696 (1960).
7. G. M. Eliashberg, Temperature Greens function for electrons in a superconductor, Sov. Phys. JETP 12, 1000 (1961).
8. W. L. McMillan, Transition temperature of strong-coupled superconductors, Phys. Rev. 167, 331 (1968).
9. M. Lüders, M. A. L. Marques, N. N. Lathiotakis, A. Floris, G. Profeta, L. Fast, A. Continenza, S. Massidda, and E. K. U. Gross, Ab initio theory of superconductivity. I. Density functional formalism and approximate functionals, Phys. Rev. B 72, 024545 (2005).
10. M. A. L. Marques, M. Lüders, N. N. Lathiotakis, G. Profeta, A. Floris, L. Fast, A. Continenza, E. K. U. Gross, and S. Massidda, Ab initio theory of superconductivity. ii. application to elemental metals, Phys. Rev. B 72, 024546 (2005).
11. A. Sanna, C. Pellegrini, and E. K. U. Gross, Combining Eliashberg Theory with Density Functional Theory for the Accurate Prediction of Superconducting Transition Temperatures and Gap Functions, Phys. Rev. Lett. 125, 057001 (2020).
12. W. A. Little, Possibility of synthesizing an organic superconductor, Phys. Rev. 134, A1416 (1964).
13. V. Ginzburg and D. Kirzhnits, On the problem of high temperature superconductivity, Phys. Rep. 4, 343 (1972).
14. D. Allender, J. Bray, and J. Bardeen, Model for an exciton mechanism of superconductivity, Phys. Rev. B 7, 1020 (1973).

15. F. P. Laussy, A. V. Kavokin, and I. A. Shelykh, ExcitonPolariton Mediated Superconductivity, Phys. Rev. Lett. 104, 106402 (2010).